ELSEVIER

International Journal of Pharmaceutics 241 (2002) 241–251

international journal of pharmaceutics

www.elsevier.com/locate/ijpharm

Prediction of passive intestinal absorption using bio-mimetic artificial membrane permeation assay and the paracellular pathway model

Kiyohiko Sugano [a],*, Noriyuki Takata [a], Minoru Machida [a], Kimitoshi Saitoh [a], Katsuhide Terada [b]

[a] *Drug Metabolism and Pharmacokinetics Laboratory, Fuji Gotemba Research Labs, Chugai Pharmaceutical Co., Ltd., 1-135 Komakado, Gotemba, Shizuoka 412-8513, Japan*

[b] *Department of Pharmaceutics, School of Pharmaceutical Sciences, Toho University, 2-2-1 Miyama, Funabashi, Chiba 274-8510, Japan*

Received 28 December 2001; received in revised form 3 April 2002; accepted 24 April 2002

Abstract

The purpose of this study was to construct and examine the prediction model for total passive permeation through the intestinal membrane. The paracellular pathway prediction model based on Renkin function (PP-RF) was combined with a bio-mimetic artificial membrane permeation assay (BAMPA), which is an in vitro method to predict transcellular pathway permeation, to construct the prediction model (BAMPA-PP-RF model). The parameters of the BAMPA-PP-RF model, e.g. apparent pore radius and potential drop of the paracellular pathway, were calculated from BAMPA permeability, the dissociation constant, the molecular radius and the fraction of a dose absorbed in humans consisting of 80 structurally diverse compounds. The apparent pore radius and the apparent potential drop obtained in this study were 5.61–5.65 Å and 75–86 mV, respectively, and these were in accordance with the previously reported values. The mean square root error of the BAMPA-PP-RF model was 13–14%. The BAMPA-PP-RF model was shown to be able to predict the total passive permeability more adequately than BAMPA alone.

Keywords: Permeability; Transcellular; Paracellular; Prediction; In silico; Artificial membrane

---

1. Introduction

Pharmacokinetics are widely recognized as an important factor in the drug discovery/development process, because many candidate compounds have been eliminated after starting clinical studies, due to inadequate absorption, distribution, metabolism, excretion or pharmacokinetics

---

* Corresponding author. Tel.: +81-550-87-6781; fax: +81-550-87-5397

E-mail address: suganokyh@chugai-pharm.co.jp (K. Sugano).

PII: S0378-5173(02)00240-5

(ADME/PK)· Therefore, the ADME/PK study is usually incorporated in the drug discovery process (Venkatesh and Lipper, 2000). Recently, the drug discovery/development process was accelerated following rapid progress in drug synthesis by combinatorial chemistry and high throughput screening based on the in vitro pharmacological assay. Therefore, the ADME/PK has remained as the bottle-neck of the drug discovery/development process, from the view point of both the success rate of clinical studies and discovery/development speed. To eliminate these problems, a 'reductionist' approach has been taken by most pharmaceutical companies. In the development of perorally administered drugs, one of the pivotal processes a drug candidate generally undergo to reach its biological target is permeation through the intestinal epithelial membrane. The permeation process could be reduced to the passive transcellular pathway, the passive paracellular pathway, and active transport pathways (both flux and efflux). Although active transport pathways have been clearly characterized, it has been difficult to delineate the extent to which a solute permeates the intestinal epithelial membrane by the paracellular and the transcellular pathway.

The parallel artificial membrane permeation assay (PAMPA) was first introduced by Kansy et al. as a rapid in vitro assay of transcellular permeation (Kansy et al., 1998). PAMPA is an application of the filter supported lipid membrane, and is completely artificial without pores and active transporter systems (Thompson et al., 1980). PAMPA is currently used by many pharmaceutical companies. Recently, bio-mimetic artificial membrane permeation assay (BAMPA) was introduced as an improved version of PAMPA (Sugano et al., 2001). In BAMPA, the composition of the lipid membrane was modified to mimic the intestinal brush border membrane. In addition, Adson et al. previously reported that the paracellular permeation could be predicted using the calculation model for molecular size-restricted diffusion within a negative electrostatic field of force (Adson et al., 1994, 1995). The Renkin function was employed as the molecular size-restriction function in their model.

The purpose of the present study was to construct a prediction model of total passive permeation through the intestinal epithelial membrane by combining BAMPA and the paracellular pathway prediction model with the Renkin-function (PP-RF), and to examine the predictability of the constructed model.

2. Theory

The permeability coefficient of the total passive transport across the intestinal epithelial membrane (P_{tot}) is the sum of the permeability coefficients of the transcellular and the paracellular pathways (P_{trans} and P_{para}, respectively) (Pade and Stavchansky, 1997):

$$P_{\mathrm{tot}} = P_{\mathrm{trans}} + P_{\mathrm{para}} \tag{1}$$

The transcellular permeability is assumed to be in proportion to the bio-mimetic artificial membrane permeability (P_{am}):

$$P_{\mathrm{tot}} = \mathrm{a}P_{\mathrm{am}} + P_{\mathrm{para}} \tag{2}$$

Adson et al. (1994) derived a systematic and quantitative approach to estimate passive transport through the paracellular pathway using several hydrophilic solutes of varying molecular size and charge. The approach utilizes the theory of molecular size-restricted diffusion within a negative electrostatic field of force. The permeability coefficient of a compound through the paracellular pathway is expressed by Eq. (3):

$$P_{\mathrm{para}} = \sum^{z} \mathrm{f}^{z} P^{z}_{\mathrm{para}} \tag{3}$$

where z is the valence of each neutral, anion and cation species (zero for neutral), f^{z} and P^{z}_{para} are the fraction and permeability of each species, respectively. The fraction of each charged species could be calculated from pK_{a}(s) of each compound (Kramer, 2001). The permeability of each charged species across the aqueous pores of the paracellular pathway are expressed by Eqs. (4) and (5):

$$P^{0}_{\mathrm{para}} = \frac{\varepsilon D}{\delta} F\left(\frac{r}{R}\right) \tag{4}$$

$$P^{z}_{\mathrm{para}} = \frac{\varepsilon D}{\delta} F\left(\frac{r}{R}\right)\left(\frac{\kappa(z)}{1 - \mathrm{e}^{\kappa(z)}}\right) \tag{5}$$

where ε is the porosity, D is the aqueous diffusion coefficient of the molecule, r is the radius of the molecule, R is the apparent radius of the pore, $F(r/R)$ is the molecular sieving factor, and κ is the dimensionless electrochemical energy function across the pore of length δ, and is estimated using Eq. (6):

$$\kappa(z) = \frac{ez|\Delta\Psi|}{k_{\mathrm{B}}T} = Cz \tag{6}$$

where, $C = e/\Delta\Psi/k_{\mathrm{B}}T$, e is the unit charge of an ion, 4.8×10^{-10} esu, $|\Delta\Psi|$ is the apparent potential drop across the barrier, k_{B} is the Boltzmann constant. 1.38×10^{-23} J/K, and T is the temperature in degrees Kelvin.

The molecular radius of the drugs were estimated from their molecular volumes using Eq. (7):

$$r = \sqrt[3]{\frac{3Vx}{4\pi} \times 166} \tag{7}$$

where, Vx is the McGowan's molecular volume ($\mathrm{cm^3/mol}$ 100) and r is the molecular radius (Abraham and McGowan, 1987). Vx can be calculated from molecular structure, using a table of atomic constants (Abraham, 1993). The molecular weights of the drugs used in this investigation were in the range of 100–650, therefore, these molecules were assumed to be spherical molecules. The aqueous diffusion coefficient (D) is estimated using the Stokes–Einstein equation for small, spherical molecules:

$$D = \frac{k_{\mathrm{B}}T}{6\pi\eta}\frac{1}{r} \times 10^{8} \tag{8}$$

where η is the viscosity of water. The dimensionless molecular sieving function, $F(r/R)$, compares the molecular radius, r, with the pore radius, R, and $0 < F(r/R) < 1$. The molecular sieving function for cylindrical channels and spherical molecules is calculated using the Renkin equation, and is expressed by Eq. (9) (Deen, 1987):

$$F\left(\frac{r}{R}\right) = \left(1 - \left(\frac{r}{R}\right)\right)^{2} \left(1 - 2.104\left(\frac{r}{R}\right) + 2.09\left(\frac{r}{R}\right)^{3} - 0.95\left(\frac{r}{R}\right)^{5}\right) \tag{9}$$

Eqs. (3)–(9) were referred as the paracellular pathway prediction model with Renkin-function (PP-RF) in this report. With Eqs. (2)–(6), one obtains:

$$P_{\mathrm{tot}} = \mathrm{a}P_{\mathrm{am}} + b\frac{1}{r}F\left(\frac{r}{R}\right)\left(f^{0} + \sum^{(z\neq 0)} f^{z}\left(\frac{Cz}{1-\mathrm{e}^{Cz}}\right)\right) \tag{10}$$

where $b = \varepsilon k_{\mathrm{B}}T/6\pi\eta\delta$. The fraction of a dose absorbed (Fa%) is a function of P_{tot} (Amidon et al., 1988):

$$\mathrm{Fa\%} = (1 - \exp(-a'P_{\mathrm{tot}}))100 \tag{11}$$

Therefore, combining Eqs. (10) and (11), the prediction equation which contains both transcellular and paracellular contributions is obtained:

$$\mathrm{Fa\%} = \left(1 - \exp\left(-a'\left(aP_{\mathrm{am}} + b\frac{1}{r}F\left(\frac{r}{R}\right)\left(f^{0} + \sum^{z(z\neq 0)} f^{z}\left(\frac{Cz}{1-\mathrm{e}^{Cz}}\right)\right)\right)\right)\right)100 \tag{12}$$

$$= \left(1 - \exp\left(-AP_{\mathrm{am}} - B\frac{1}{r}F\left(\frac{r}{R}\right)\left(f^{0} + \sum_{f}{}^{z}\left(\frac{Cz}{1-\mathrm{e}^{Cz}}\right)z(z=0)\right)\right)\right)100$$

where $a \times a' = A$, $b \times a' = B$. In this equation, Fa%, P_{am}, r, z and f^{z} could be measured or calculated for each compound. Therefore, by a multiple non-linear regression of Eq. (12), R, A, B and C could be determined.

3. Materials and methods

3.1. Materials

L-α-phosphatidylserine (PS), L-α-phosphatidylinositol (PI), and cholesterol (CHO) were purchased from Sigma Chemical (St. Louis, MO). L-α-phosphatidylcholine (PC) and L-α-phosphatidylethanolamine (PE) were purchased from Nippon Oil & Fats Corporation (Tokyo, Japan). 1,7-Octadien was purchased from Tokyo Kasei Kogyo (Tokyo, Japan). All generic drugs were purchased from Sigma Chemical, Tokyo Kasei Kogyo, Aldrich Chemical Company (Milwaukee, WI), Tocris Cookson (Northpoint, UK) and Alexis Corporation (San Diego, CA), except for sumatriptan and pravastatin which were extracted from marketed formulations. 4-Fluoro-7-nitrobenzofurazan (NBD-F) was purchased from Wako Pure Chemicals Industries (Tokyo, Japan). The hydrophobic filter plate (Durapore, pore size 0.45 μm) was purchased from Millipore Corporation (Bedford, MA).

3.2. Permeability studies

Permeability studies were performed in the same manner as described previously (Kansy et al., 1998; Sugano et al., 2001). A 96-well microplate (acceptor compartment) was completely filled with pH 6.0 50 mM sodium phosphate buffer containing 5% DMSO. A hydrophobic filter plate (donor compartment) was fixed on the buffer filled plate. The filter surface was impregnated with 5 μL lipid solution, which was composed of PC (0.8%)/PE (0.8%)/PS (0.2%)/PI (0.2%)/CHO (1.0%)/1,7-octadiene (97.0%). 1,7-Octadiene is an irritant and inhalation should be avoided. A 0.5 mM sample stock solution (100 μl) of the same buffer was added to the filter plate and incubated at 30 °C for 2 or 15 h. The filter plate was carefully removed. Reference solutions were prepared by diluting the sample stock solution to the same concentration as that with no membrane barrier. Most compounds were quantified by UV spectroscopy, using the microtiter plate reader Spectramax 190 (Molecular Devices) at 240–440 nm at intervals of 10 nm. Lactulose and Raffinose were quantified by the standard phenol sulfate method (Dubois et al., 1956). Ethambutol and tranexamic acid were quantified by the standard NBD-F fluorescence method (Watanabe and Imai, 1981). Lincomycin was quantified by LC–MS (micromass ZQ-alliance 2790 separation module, Waters) using a C18 column (Xterra MS-C18 3.5 μm 2.1 × 30 mm, Waters), and an acetonitrile/0.01 M ammonium acetate mobile phase in linear gradient from 0 to 90% acetonitrile for 3 min. P_{am} was calculated using Eq. (13).

$$P_{\mathrm{am}} = -2.303 \times \frac{V_{\mathrm{dn}} \times V_{\mathrm{ac}}}{V_{\mathrm{dn}} + V_{\mathrm{ac}}} \times \frac{1}{S \times t} \times \log\left(1 - \frac{\mathrm{flux\%}}{100}\right) \tag{13}$$

$$\mathrm{flux\%} = \frac{\mathrm{OD}_{\mathrm{ac}}}{\mathrm{OD}_{\mathrm{ref}}} \times 100 \tag{14}$$

V_{dn} (ml), volume of the donor compartment (0.1 ml); V_{ac} (ml), volume of the acceptor compartment (0.38 ml); $\mathrm{OD}_{\mathrm{ac}}$, optical density of the solution of the acceptor compartment; $\mathrm{OD}_{\mathrm{ref}}$, optical density of the reference solution; S (cm^2), membrane area (0.266 cm^2); t (s), incubation time.

3.3. Non-linear regression analysis

Curve fitting and correlation coefficients were calculated by the least-square method (EXCEL 2000, Microsoft, Redmont, WA). Sum of squares of the difference between calculated Fa% ($\mathrm{Fa\%}_{\mathrm{calc}}$) and observed Fa% ($\mathrm{Fa\%}_{\mathrm{obs}}$) was minimized using the Quasi–Newton method to obtain each coefficient of Eq. (12).

4. Results and discussion

4.1. Construction of the BAMPA-PP-RF model Eq. (12)

It is well known that tight junction (TJ) play an important role for restricting the movement of the compounds across the paracellular pathway. Freeze-fracture electron micrographs of the constrictive region of the TJ show netlike arrays of strands (made partly of the cytoskeleton) circumscribing the cell, forming a division between the apical and the basolateral sides (Anderson, 2001). Permeation through the paracellular pathway can be modeled as molecular size-restricted diffusion within a negative electrostatic field of force, and expressed as Eqs. (3)–(9) (PP-RF). The PP-RF is combined with P_{am}, and finally, Eq. (12) is obtained as the BAMPA-PP-RF model for the prediction of total passive permeability. The P_{am} of structurally diverse compounds, with a molecular radius (r) in the range of 3.18–5.62 Å and different net charges in the range of -2 to $+2$, were measured by BAMPA. We mainly selected compounds whose Fa% was less than 90%, because prediction of this range of Fa% is anticipated for the in vitro method in the drug discovery process. Compounds which are known to be actively transported were excluded (Swaan and Tukker, 1995; Döppenschmitt et al., 1998; Bretschneider et al., 1999). P_{am} was plotted against Fa% in Fig. 1.

Each coefficient of Eq. (12) was calculated by non-linear regression analysis using, Fa%, P_{am}, r, z and f^z of each compound. When the P_{am} was less than the detection limit, the detection limit value was used as P_{am}. In all cases, the detection limit of P_{am} was lower than 2.67×10^{-7} cm/s which corresponds to the transcellular $\mathrm{Fa\%_{calc}} <$ 6% (described later). Therefore, the contribution of P_{am} to the regression analysis could be neglected. Mannitol, erythritol and creatinine, which were known as paracellular solute, were also included in the analysis (P_{am} was assumed to be 1×10^{-8} cm/s) (Karlsson et al., 1999). The coefficients of Eq. (12) are shown in Tables 1 and 2.

In Fig. 2A, $\mathrm{Fa\%_{calc}}$ calculated by Eq. (12) with coefficient set 1 in Table 2, was plotted against $\mathrm{Fa\%_{obs}}$. Practolol was found to be the outliner ($\mathrm{Fa\%_{calc}} = 54\%$, $\mathrm{Fa\%_{obs}} = 100\%$). The permeability of practolol in vivo (rat in situ) was reported to be less than that of sotalol whose $\mathrm{Fa\%_{obs}}$ was 60% (Taylor et al., 1985). Therefore, analysis without practolol was also performed (Table 2, set 3). The R and $|\Delta\Psi|$ obtained in this study were 5.61–5.65 Å and 75–86 mV, respectively. Previously, R was reported to be 6.7–8.8 Å in human jejunum and 5.2–12.0 Å in Caco-2 cell, and $|\Delta\Psi|$ was reported to be 18–57 mV in Caco-2 cell (the

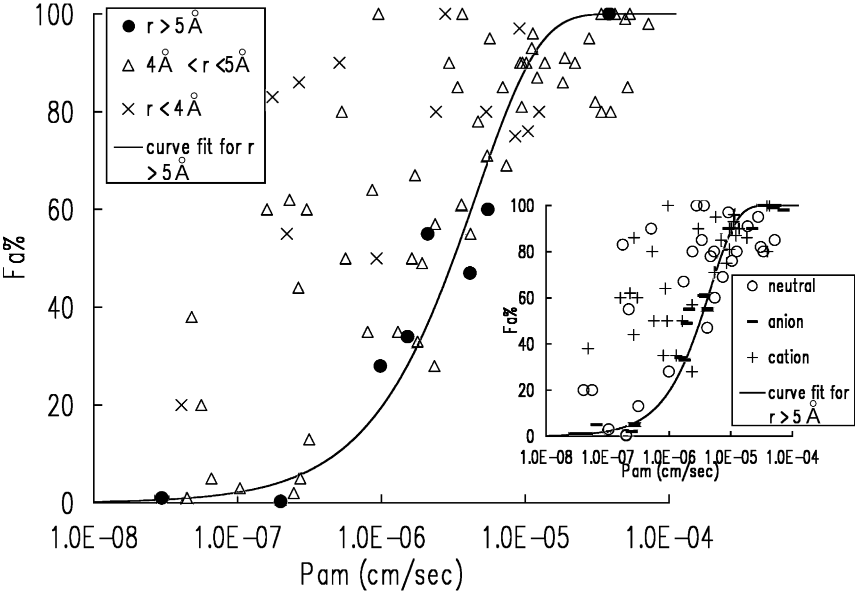

Fig. 1. The fraction of a dose absorbed in humans (Fa%) vs. P_{am} measured with PC (0.8%)/PE (0.8%)/PS (0.2%)/PI (0.2%)/CHO (1.0%)/1,7-octadiene membrane at pH 6.0. The detection limit values were used with compounds whose P_{am} were less than the detection limit. The curved line in the figure is the fitting line of (Eq. (12)) for the molecule with molecular radius (r) > 5 Å (Table 2, set 2). Values represent the means of three experiments. In the main figure, compounds were classified by molecular radius. The insert shows the classification by charge.

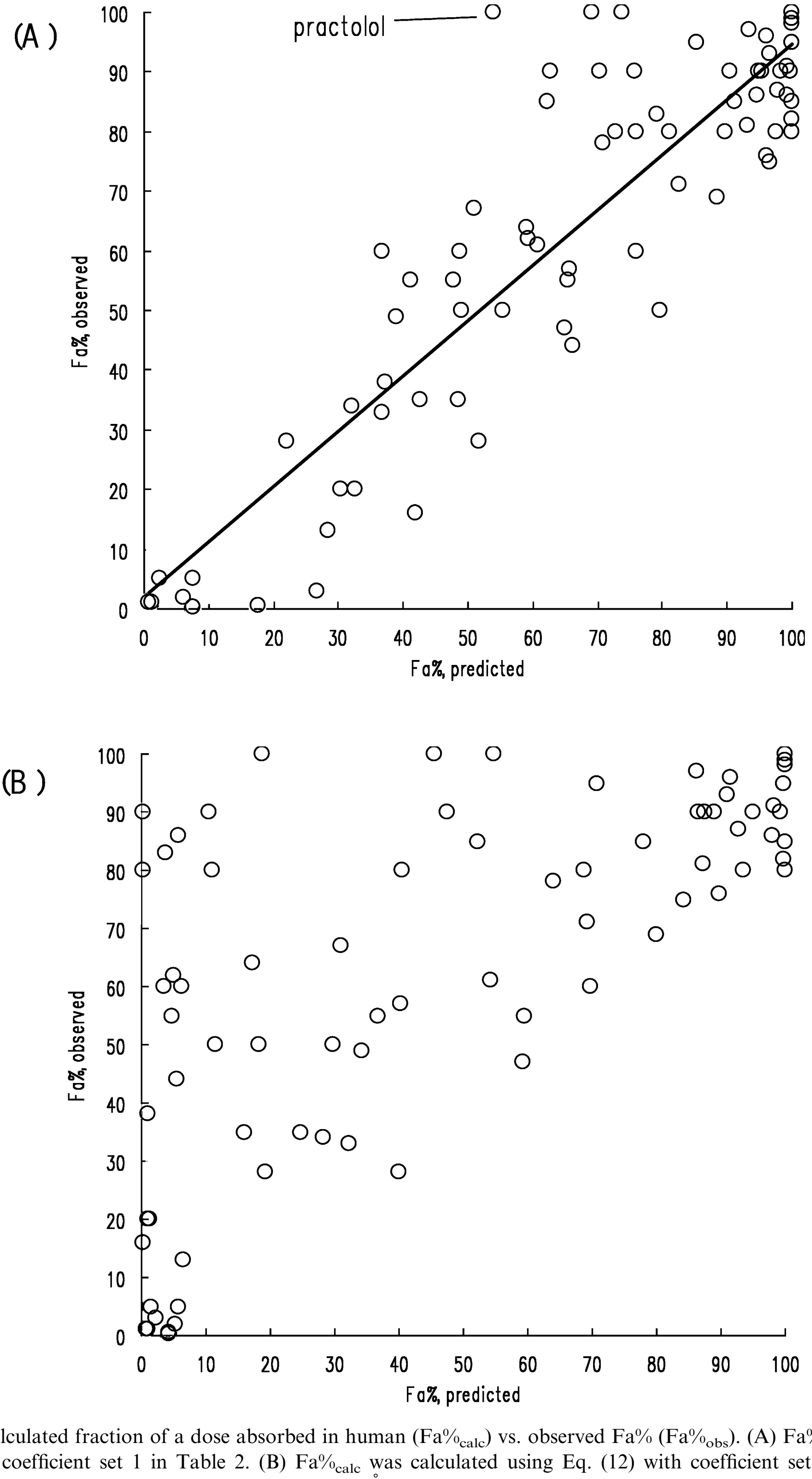

Fig. 2. Plot of the calculated fraction of a dose absorbed in human (Fa$\%_{calc}$) vs. observed Fa% (Fa$\%_{obs}$). (A) Fa$\%_{calc}$ was calculated using Eq. (12) with coefficient set 1 in Table 2. (B) Fa$\%_{calc}$ was calculated using Eq. (12) with coefficient set 2 in Table 2. The coefficient set 2 was calculated with the compounds of $r > 5$ Å.

Table 1
Fa%, P_{am} and molecular properties

Number	Compound	Fa%[a]	P_{am} ($\times 10^{-6}$ cm/s)[b]	Vx (cm^3/mol per 100)	MW[c]	r (Å)	pK_a[d]	Fa%$_{calc}$[e]
1	Acebutolol	90	2.95 ± 0.26	2.76	336	4.78	9.4 (b)	63
2	Acetaminophen	80	2.39 ± 0.96	1.17	151	3.59		73
3	Acyclovir	20	<0.04[f]	1.52	225	3.92		33
4	Allopurinol	90	0.51 ± 0.29	0.88	136	3.27		76
5	Alprenolol	93	11.1 ± 0.5	2.16	249	4.41	9.65 (b)	97
6	Ailoride	50	0.93 ± 0.08	1.51	230	3.91	8.7 (b)	80
7	Antipyrine[g]	97	9.12 ± 0.70	1.48	188	3.89		93
8	Atenolol	50	0.56 ± 0.11	2.18	266	4.42	9.6 (b)	49
9	Aztreonam	1	<0.04[f]	2.76	435	4.78	−0.70 (a), 2.75 (a)	1
10	Bromocriptine	28	0.99 ± 0.17	4.48	654	5.62	5.87 (b)	22
11	Bupropion	87	12.1 ± 2.6	1.94	240	4.25	8.35 (b)	98
12	Ceftriaxone	1	0.03 ± 0.02	3.48	554	5.17	3.2 (a), 4.1 (a)	1
13	Cefuroxime	5	0.07 ± 0.01	2.73	424	4.76	2.45 (a)	3
14	Chloramphenicol[g]	90	22.1 ± 0.6	2.07	323	4.34	5.5 (a)	100
15	Chlorothiazide	13	0.31 ± 0.20	1.69	296	4.06	6.7 (a)	28
16	Cimetidine	64	0.86 ± 0.16	1.96	252	4.27	7.11 (b)	59
17	Ciprofloxacin	69	7.39 ± 0.33	2.30	331	4.50	6.0 (a), 8.8 (b)	89
18	Cloxacillin	49 (37–60)	1.92 ± 0.55	2.89	436	4.85	2.7 (a)	39
19	Creatinine	80	–[h]	0.84	113	3.21	4.85 (b)	81
20	Cymarin	47	4.13 ± 1.34	4.08	548	5.45		65
21	Cytarabine	<20	<0.06[f]	1.62	243	4.01	4.35 (b)	30
22	Dexamethasone[g]	80	33.9 ± 0.3	2.91	392	4.87		100
23	Diclofenac	100	53.3 ± 0.7	2.03	296	4.32	4.0 (a)	100
24	Dicloxacillin	55 (35–76)	4.16 ± 1.22	3.01	470	4.92	2.75 (a)	65
25	Dilthiazem[g]	80	39.3 ± 0.8	3.14	415	4.99	7.7 (b)	100
26	Doxycycline[g]	95 (90–100)	27.8 ± 0.3	3.10	444	4.97	3.4 (a), 9.7 (b)	100
27	Erythritol	90	–	0.91	122	3.30		70
28	Ethambutol	80	0.53 ± 0.14	1.83	204	4.17	6.1 (b), 9.2 (b)	76
29	Ethionamide	80	12.5 ± 2.0	1.32	166	3.74		98
30	Famotidine	38	<0.05[f]	2.26	337	4.47	7.1 (b)	37
31	Fenoterol	60	<0.16[f]	2.36	303	4.54	8.5 (b)	37
32	Flecainide	81	9.44 ± 0.71	2.60	414	4.69	9.3 (b)	93
33	Flucytosin	83 (75–90)	0.18 ± 0.13	0.81	129	3.18		79
34	Furosemide	61	3.60 ± 0.08	2.10	330	4.37	3.9 (a)	61
35	Ganciclovir	3	0.10 ± 0.06	1.72	255	4.08		27
36	Guanabenz[g]	75	8.52 ± 0.66	1.56	231	3.95	8.1 (b)	97
37	HBED	5	0.27 ± 0.05	2.92	388	4.87	4.64 (a)	7
38	Hdrochlorothiazide	67	1.71 ± 0.06	1.73	298	4.09		51
39	Hydrocortisone[g]	91	18.8 ± 0.6	2.80	362	4.81		99
40	Imipramine[g]	100	42.1 ± 0.2	2.40	280	4.56	9.5 (b)	100
41	Ioniazid	80	5.35 ± 2.31	1.03	137	3.44		90
42	Ketoprofen[g]	100	33.8 ± 2.1	1.98	254	4.28	3.89 (a)	100
43	Lactulose	0.6	<0.20[f]	2.23	342	4.45		18
44	Lansoprazole	85	3.39 ± 0.08	2.37	369	4.55		62
45	Lincomycin	28	2.34 ± 1.26	3.10	406	4.97	7.6 (b)	52
46	Mannitol	16	–	1.31	182	3.73		42
47	Metaproterenol	44	<0.26[f]	1.70	211	4.07	8.6 (b)	66
48	Metformin	86	<0.27[f]	1.09	129	3.51	12.4 (b)	95

Table 1 *(Continued)*

Number	Compound	Fa%[a]	P_{am} ($\times 10^{-6}$ cm/s)[b]	*Vx* (cm^3/mol per 100)	MW[c]	*r* (Å)	pK_a[d]	Fa%$_{\mathrm{calc}}$[e]
49	Methylprednisolone	82	30.7 ± 1.1	2.90	374	4.86		100
50	Metoprolol	95	5.67 ± 0.55	2.26	267	4.47	9.68 (b)	85
51	Nadolol	35	0.80 ± 0.19	2.49	309	4.62	9.67 (b)	43
52	Naltrexone	96	11.3 ± 2.0	2.44	341	4.59	8.13 (b)	96
53	Naproxen[g]	99	49.5 ± 3.2	1.78	230	4.13	4.15 (a)	100
54	Norfloxacin	71	5.43 ± 0.75	2.27	319	4.48	6.34 (a), 8.75 (b)	83
55	Olsalazine	2	0.25 ± 0.02	2.03	302	4.32	3.06 (a), 3.06 (a)[i]	6
56	Oxacillin	33 (30–35)	1.78 ± 0.28	2.76	401	4.78	2.8 (a)	37
57	Oxytetracycline	60	5.49 ± 0.15	3.16	460	5.00	3.3 (a), 9.1 (b)	76
58	Pindolol[g]	90	9.56 ± 0.22	2.01	248	4.30	8.8 (b)	95
59	Practolol	100	0.95 ± 0.55	2.18	266	4.42	9.5 (b)	54
60	Pravastatin	34	1.52 ± 0.16	3.37	425	5.11	4.2 (a)	32
61	Prazosin[g]	86 (77–95)	18.2 ± 1.1	2.74	383	4.77	7.04 (b)	99
62	Procainamide	85 (75–95)	6.97 ± 0.41	2.02	235	4.31	9.23 (b)	91
63	Propranolol[g]	90	13.7 ± 1.4	2.15	259	4.40	9.52 (b)	98
64	Propylthiouracil	76	10.4 ± 5.1	1.28	170	3.70		96
65	Raffinose	0.3	<0.20[f]	3.26	504	5.06		8
66	Ranitidine	50	1.63 ± 0.03	2.40	314	4.56	8.2 (b)	55
67	Sotalol	60	0.30 ± 0.09	2.10	272	4.37	9.8 (b)	49
68	Sulindac	90	9.20 ± 1.34	2.57	356	4.67	4.7 (a)	90
69	Sulpiride	35	1.30 ± 0.62	2.53	341	4.65	9 (b)	48
70	Sumatriptan	57	2.36 ± 0.23	2.27	295	4.48	9.63 (b)	66
71	Terbutaline	62	<0.23[f]	1.84	225	4.18	8.72 (b)	59
72	Tetracycline	78 (75–80)	4.70 ± 0.16	3.10	444	4.97	3.3 (a), 9.5 (b)	71
73	Theophylline	100	2.78 ± 2.23	1.22	180	3.64		74
74	Timolol[g]	90	10.2 ± 1.3	2.38	316	4.55	9 (b)	95
75	Tolbutamide	85	51.5 ± 5.8	2.06	270	4.34	5.3 (b)	100
76	Tranexamic acid	55	0.22 ± 0.17	1.30	157	3.72	4.51 (a), 10.72 (b)	48
77	Valsartan	55	2.10 ± 1.12	3.41	436	5.13	3.9 (a), 4.7 (a)	41
78	Verapamil[g]	100	38.4 ± 0.9	3.79	455	5.32	8.66 (b)	100
79	Warfarin[g]	98	72.0 ± 1.2	2.31	308	4.51	5.03 (a)	100
80	Zidovudine	100	3.65 ± 0.73	1.82	267	4.16		69

[a] Fa% (the fraction of a dose absorbed in humans) values were obtained from previously reported values (Noel, 1979; McEvoy, 1998; Wessel et al., 1998; Winiwarter et al., 1998). When the Fa% value was reported as a range, the mid-value of the range was used (Parenthesis indicating range).

[b] Artificial membrane permeability coefficient measured with the PC (0.8%)/PE (0.8%)/PS (0.2%)/PI (0.2%)/CHO (1.0%)/1,7-octadiene membrane at pH 6.0. Values are represented as the mean ± S.D. The assays were performed in triplicate. The incubation time was 15 h, or otherwise noted.

[c] Molecular weight.

[d] Obtained from various sources, mainly from McEvoy, 1998. The pK_a values of the acid (p$K_a < 7.3$) and base (p$K_a > 4.7$) are indicated (parenthesis indicating acid (a) and base (b)).

[e] Fa% calculated using Eq. (12) with coefficient set 1 in Table 2.

[f] Less than the detection limit. Detection limit was set at $OD_{\mathrm{ac}} = 0.005$.

[g] The incubation time was 2 h.

[h] Not determined.

[i] The two pK_as of carboxylic acid were assumed to be equal.

Table 2
R, $|\Delta\Psi|$, A and B of Eq. (12)

Number	Compound set[a]	n	R (Å)	$\|\Delta\Psi\|$ (mV)[b]	A ($\times 10^5$)	B ($\times 10^2$)	CC[c]	RMSE[d]
1	All compounds	80	5.65	86	2.53	1.87	0.895	14
2	$r > 5$ Å[e]	8	–[f]	–	2.18	–	0.957	9
3	Practolol	79	5.61	75	2.50	1.95	0.909	13

[a] Compounds employed to calculate the coefficients of Eq. (12).
[b] Coefficient C was converted to $|\Delta\Psi|$ using Eq. (6).
[c] Correlation coefficient between $\text{Fa\%}_{\text{calc}}$ and $\text{Fa\%}_{\text{obs}}$.
[d] Root mean square error between $\text{Fa\%}_{\text{calc}}$ and $\text{Fa\%}_{\text{obs}}$ of the compounds employed.
[e] Compounds with a molecular radius larger than 5 Å were employed.
[f] Not determined.

latter $|\Delta\Psi|$ value was calculated from the previously reported values) (Seorgel, 1993; Adson et al., 1994; Knipp et al., 1997). Therefore, the R and $|\Delta\Psi|$ obtained in this study were in accordance with the previously reported values.

4.2. Predictability of BAMPA-PP-RF model

To clarify the contribution of the paracellular pathway to the predictability of the model, a prediction without PP-RF was performed (Fig. 2B). In this case, $B = 0$ and A was obtained with the transcellular solute ($r > 5$ Å) (Table 2, set 2). Combining BAMPA and PP-RF, the predictability was improved. By BAMPA alone, small neutral and cationic compounds were underestimated (Figs. 1 and 2B).

The mean square root error of the BAMPA-PP-RF model was 13–14% and appeared to be small enough for use during the early stages of the drug discovery/development process. In PP-RF, the only two solute descriptors, r and z, were used to describe the interaction between solute and TJ, and the pore radius of TJ was theoretically assumed to be uniform. There have been several studies suggesting that some properties of compounds other than r and z influence the paracellular permeation (Kristl and Tukker, 1998; Sugano et al., 2000). In addition, the Renkin function is quantitatively satisfactory for $0 < F(r/R) < 0.4$. Therefore, the PP-RF should be taken as a first approximation. Previously, the adaptability of PP-RF was confirmed merely for several compounds. Therefore, it is noteworthy that PP-RF was found to be able to predict the contribution of the paracellular pathway adequately for several dozen compounds in the present study. With more in vivo and/or in vitro absorption findings, which include both the transcellular and paracellular pathway, and P_{am} data, the paracellular pathway prediction model could be improved further. To predict P_{para} by PP-RF, one needs to obtain the data of r and z. In this study, the measured pK_a(s) data were obtained from the literature, and r was calculated manually from the compound structure. Computer programs are commercially available to calculate the pK_a(s) and r from the structural information using the automatic batch process. Therefore, PP-RF can be used as an in silico method for the prediction of $P_{\text{para.}}$ If the in silico prediction of BAMPA is established in the future, the total passive permeability, as well as the contribution ratio of both pathways, would become predictable in silico.

5. Conclusions

In this study, the BAMPA-PP-RF model was shown to be able to predict the total passive permeability more adequately than BAMPA alone. Usually, the in vivo method and cell based in vitro method, which contain several permeation pathways, are used in the drug design program, and findings obtained by these methods have been previously used to construct the in silico method (Ekins et al., 2000). Therefore, it is difficult to pinpoint which of the compound's properties should be optimized in the drug design program.

The advantage of the BAMPA-PP-RF model would be that the permeability of transcellular and paracellular pathway is estimated separately, and combined to predict the total passive absorption. Therefore, the permeability was easily elucidated by the compound's structure. The 'reductionist' approach, as shown in this study, would enable the fast, precise and comprehensive approach for the prediction of oral absorption during the drug discovery/development process.

References

Abraham, M.H., 1993. Scales of solute hydrogen-bonding: their construction and application to physicochemical and biochemical processes. Chem. Soc. Rev. 22, 73–83.

Abraham, M.H., McGowan, J.C., 1987. The use of characteristic volumes to measure cavity terms in reversed phase liquid chromatography. Chromatographia 23, 243–246.

Adson, A., Ruab, T.J., Burton, P.S., Barsuhn, C.L., Hilgers, A.R., Audus, K.L., Ho, N.F.H., 1994. Quantitative approaches to delineate paracellular diffusion in cultured epithelial cell monolayers. J. Pharm. Sci. 83, 1529–1530.

Adson, A., Burton, P.S., Ruab, T.J., Barsuhn, C.L., Audus, L., Ho, N.F.H., 1995. Passive diffusion of weak organic electolytes across Caco-2 cell monolayers: Uncoupling the contributions of hydrodynamic, transcellular and paracellular barriers. Pharm. Res. 84, 1197–1203.

Amidon, G.L., Sinko, P.J., Fleisher, D., 1988. Estimating human oral fraction dose absorbed, a correlation using rat intestinal membrane permeability for passive and carrier-mediated compounds. Pharm. Res. 5, 651–654.

Anderson, J.M., 2001. Molecular structure of tight junctions and their role in epithelial transport. News Physiol. Sci. 16, 126–130.

Bretschneider, B., Brandsch, M., Neubert, R., 1999. Intestinal transport of beta-lactam antibiotics: analysis of the affinity at the H+/peptide symporter (PEPT1), the uptake into Caco-2 cell monolayers and the transepithelial flux. Pharm. Res. 16, 55–61.

Deen, W.M., 1987. Hindered transport of large molecules in liquid-filled pores. Am. Inst. Chem. Eng. J. 33, 1409–1425.

Döppenschmitt, S., Spahn-Langguth, H., Regardh, C.G., Langguth, P., 1998. Radioligand-binding assay employing *P*-glycoprotein-overexpressing cells: testing drug affinities to the secretory intestinal multidrug transporter. Pharm. Res. 15, 1001–1006.

Dubois, M., Gilles, K.A., Hamilton, J.K., Rebers, P.A., Smith, F., 1956. Colorimetric method for determination of sugars and related substances. Anal. Chem. 28, 350–356.

Ekins, S., Waller, C.L., Swaan, P.W., Cruciani, G., Wrighton, S.A., Wikel, J.H., 2000. Progress in predicting human ADME parameters in silico. J. Pharm. Toxicol. Methods 44, 251–272.

Kansy, M., Senner, F., Gubernator, K., 1998. Physicochemical high throughput screening: parallel artificial membrane permeation assay in the description of passive absorption processes. J. Med. Chem. 41, 1007–1010.

Karlsson, J., Ungell, A.l., Grasjo, J., Artursson, P., 1999. Paracellular drug transport across intestinal epithelia: influence of charge and induced water flux. Eur. J. Pharm. Sci. 9, 47–56.

Knipp, T.G., Ho, N.F.H., Barsuhn, C.L., Borchardt, R.T., 1997. Paracellular diffusion in Caco-2 cell monolayers: effect of perturbation on the transport of hydrophilic compounds that vary in size and charge. J. Pharm. Sci. 86, 1105–1110.

Kramer, S.D., 2001. Liposome/water partitioning: theory, techniques, and applications. In: Testa, B., van de Waterbeend, H., Folkers, G., Guy, R. (Eds.), Pharmacokinetic Optimization in Drug Research. Verlag Helvetica Chimica Acta Wiley-VCH, Zurich, Weinheim, pp. 401–428.

Kristl, A., Tukker, J.J., 1998. Negative correlation of *n*-octanol/water partition coefficient and transport of some guanine derivatives through rat jejunum in vitro. Pharm. Res. 15, 499–501.

McEvoy, G.K. (Ed.), 1998. AHFS Drug Information. American Society of Health-system Pharmacist, Bethesda, MD.

Noel, M., 1979. Kinetic study of normal and sustained release dosage forms of metformin in normal subjects. Res. Clin. Forums 1, 33–44.

Pade, V., Stavchansky, V., 1997. Estimation of the relative contribution of the transcellular and paracellular pathway to the transport of passively absorbed drugs in the Caco-2 cell culture model. Pharm. Res. 14, 1210–1215.

Seorgel, K.H., 1993. Showdown at the tight junction. Gastroenterology 105, 1247–1250.

Sugano, K., Yoshida, S., Takaku, M., Haramura, M., Saitoh, R., Nabuchi, Y., Ushio, H., 2000. Quantitative structure-intestinal permeability relationship of benzamidine analogue thrombin inhibitor. Bioorg. Med. Chem. Lett. 10, 1939–1942.

Sugano, K., Hamada, H., Machida, M., Ushio, H., 2001. High throughput prediction of oral absorption: improvement of the composition of the lipid solution used in parallel artificial membrane permeation assay. J. Biomol. Screen. 6, 189–196.

Swaan, P.W., Tukker, J.J., 1995. Carrier mediated transport mechanism of foscarnet (trisodium phosphonoformate hexahydrate) in rat intestinal tissue. J. Pharmacol. Exp. Ther. 272, 242–247.

Taylor, D.C., Pownall, R., Burke, W., 1985. The absorption of beta-adrenoceptor antagonists in rat in-situ small intestine; the effect of lipophilicity. J. Pharm. Pharmacol. 37, 280–283.

Thompson, M., Krull, U.J., Worsfold, P.J., 1980. The structure and electrochemical properties of a polymer-supported lipid biosenser. Anal. Chim. Acta 117, 133–145.

Venkatesh, S., Lipper, R.A., 2000. Role of the development scientist in compound lead selection and optimization. J. Pharm. Sci. 89, 145–154.

Watanabe, Y., Imai, K., 1981. High-performance liquid chromatography and sensitive detection of amino acids derivatized with 7-fluoro-4-nitrobenzo-2-oxa-1,3-diazole. Anal. Biochem. 116, 471–472.

Wessel, M.D., Jurs, P.C., Tolan, J.W., Muskal, S.M., 1998. Prediction of human intestinal absorption of drug compounds from molecular structure. J. Chem. Inf. Comput. Sci. 38, 726–735.

Winiwarter, S., Bonham, N.M., Ax, F., Hallberg, A., Lennernas, H., Karlen, A., 1998. Correlation of human jejunal permeability (in vivo) of drugs with experimentally and theoretically derived parameters. A multivariate data analysis approach. J. Med. Chem. 41, 4939–4949.